MULTIFREQUENCY RADIO OBSERVATIONS OF A SNR IN THE LMC. THE CASE OF SNR J0527–6549 (DEM L204)

L. M. Bozzetto, M. D. Filipović, E. J. Crawford, I. S. Bojičić, J. L. Payne,

A. Mendik, B. Wardlaw and A. Y. De Horta

School of Computing and Mathematics, University of Western Sydney
Locked Bag 1797, Penrith South DC, NSW 1797, Australia

E–mail: *m.filipovic@uws.edu.au*

SUMMARY: We present a detailed study and results of new Australia Telescope Compact Array (ATCA) observations of supernova remnant SNR J0527–6549. This Large Magellanic Cloud (LMC) object follows a typical supernova remnant (SNR) horseshoe morphology with a diameter of D=(66×58)±1 pc which is among the largest SNRs in the LMC. Its relatively large size indicates older age while a steeper than expected radio spectral index of $\alpha=-0.92\pm0.11$ is more typical of younger and energetic SNRs. Also, we report detections of regions with a high order of polarization at a peak value of ~54%±17% at 6 cm.

Key words. ISM: supernova remnants – Magellanic Clouds – Radio Continuum: ISM – Polarization – ISM: individual objects: SNR J0527–6549

1. INTRODUCTION

The Large Magellanic Cloud (LMC) contains one of the most vigorous star forming regions, (such as 30 Dor) in our Local Group of galaxies. Located at a distance of 50 kpc (Di Benedetto 2008), it is one of the best galaxies to study supernova remnants (SNRs) due to the favourable position in the direction toward the South Pole. As well as its viewing position, the LMC is also located in one of the coldest areas of the radio sky which allows us to observe radio emission without the interruption from Galactic foreground radiation. In addition to this, the LMC resides outside of the Galactic plane and, therefore, the influence of dust, gas and stars is negligible.

Predominately non-thermal emission is a well-known characteristic of SNRs in the radio-continuum. Although SNRs have a typical radio spectral index of $\alpha \sim -0.5$ defined by $S \propto \nu^\alpha$, this can significantly change, due to the fact of the wide variety of types of SNRs in various environments (Filipović et al. 1998a). The ISM's morphology, structure, behaviour and evolution can be attributed to SNRs and, in turn, this heavily impacts the evolution of SNRs, as they are dependant on the environment in which they reside.

Here, we report on new radio-continuum and optical observations of previously, poorly studied, SNR J0527–6549. The observations, data reduction and imaging techniques are described in Section 2. The astrophysical interpretation of newly obtained moderate-resolution total intensity and polarimetric image in combination with the existing Magellanic Cloud Emission Line Survey (MCELS) images is discussed in Section 3.

2. OBSERVATIONAL DATA

2.1. Previous observations of SNR J0527–6549

SNR J0527–6549 was initially classified as an SNR based on the Einstein X-ray survey by Long et al. (1981) (named LHG 39). Mathewson et al. (1983) catalogued SNR J0527–6549 based on their optical observations reporting an estimated optical size of $237'' \times 212''$ ($57 \times 51 \pm 1$ pc; using 50 kpc as the distance to the LMC). They also studied this object using MOlonglo Synthesis Telescope (MOST) survey. This SNR showed in Clarke et al. (1976) 408 MHz MC4 catalogue as a distinctive point-like radio source whose integrated flux density was later re-measured by Mathewson et al. (1983) to be of 260 mJy. Mills et al. (1984) detected this source with specific MOST pointings and indicated a spectral index α=–0.45. However, Filipović et al. (1998b) reported a flatter spectral index α=–0.2±0.1.

An optically identified object at this position was also listed in the Davies et al. (1976) catalogue of nebular complexes in the Magellanic Clouds as emission nebulae — DEM L204. Chu and Kennicutt (1988) classified SNR J0527–6549 to belong to Population II? (with '?' indicating uncertain classification) group with very distant (non-influential) stellar association of LH 53 at some 340 pc. Filipović et al. (1998b), using *ROSAT* All Sky Survey (RASS) observations, detected X-ray emission from SNR J0527–6549 (LMC RASS 213). Filipović et al. (1998a) added a further confirmation with a set of single dish Parkes radio-continuum observations on a wide frequency range (Filipović et al. 1995, 1996). Blair et al. (2006) reported a marginal detection only in C III at far ultraviolet wavelengths based on FUSE (Far Ultraviolet Spectroscopic Explorer) satellite. Finally, Haberl and Pietsch (1999) (named SNR as HP 180) discuss the X-Ray properties of SNR J0527–6549 based on ROSAT PSPC observations. Most recently, Payne et al. (2008) presented optical spectroscopy of a wide range of LMC SNRs including SNR J0527–6549. They found an enhanced [S II]/H$_\alpha$ ratio of 0.8 typical of SNRs.

2.2. New observations of SNR J0527–6549

We observed SNR J0527–6549 with the Australia Telescope Compact Array (ATCA) on 2nd October 1997 using the array configuration EW375 at wavelengths of 3 and 6 cm (ν=8640 and 4800 MHz). Baselines formed with the 6th ATCA antenna were excluded, as the other five antennas were arranged in a compact configuration. The observations were carried out in the so called "snap-shot" mode, totaling ∼1 hour of integration over a 12 hour period. Source PKS B1934-638 was used for the primary calibration and source PKS B0530-727 was used for the secondary (phase) calibration. The MIRIAD (Sault and Killeen 2010) and KARMA (Gooch 2006) software packages were used for reduction and analysis. More information on the observing procedure and other sources observed in this session/project can be found in Bojičić et al. (2007), Crawford et al. (2008a,b,

2010) and Čajko et al. (2009).

Images were formed using the MIRIAD multi-frequency synthesis (Sault and Wieringa 1994) and natural weighting. They were deconvolved using the CLEAN and RESTOR algorithms with the primary beam correction applied using the LINMOS task. A similar procedure was used for both U and Q Stokes parameter maps. Because of the low dynamic range (signal to noise ratio between the source flux and 3σ noise level) self-calibration could not be applied. The 6 cm image (Fig. 1) has a resolution $41.4'' \times 30.3''$ at PA=0° and an estimated r.m.s. noise 0.15 mJy/beam. Similarly, we made an image of SNR J0527–6549 at 3 cm (Fig. 1) with resolution $22.9'' \times 16.5''$ (PA=0°).

We also used the Magellanic Cloud Emission Line Survey (MCELS) that was carried out with the 0.6 m University of Michigan/CTIO Curtis Schmidt telescope, equipped with a SITE 2048 × 2048 CCD, which gave a field of 1.35° at a scale of 2.4″ pixel^{-1}. Both the LMC and SMC were mapped in narrow bands corresponding to Hα, [O III] (λ=5007 Å), and [S II] (λ=6716, 6731 Å), plus matched red and green continuum bands that are used primarily to subtract most of the stars from the images to reveal the full extent of the faint diffuse emission. All the data have been flux-calibrated and assembled into mosaic images, a small section of which is shown in Figs. 2 and 3. Further details regarding the MCELS are given by Smith et al. (2006) and at http://www.ctio.noao.edu/mcels. Here, for the first time, we present optical images of this object in combination with our new radio- continuum data.

3. RESULTS AND DISCUSSION

The remnant has a typical horseshoe morphology (Fig. 1) centered at RA(J2000)=$5^h27^m54.9^s$, DEC(J2000)=–65°49′49.2″ with a measured diameter of $271'' \times 240'' \pm 4''$ ($66 \times 58 \pm 1$ pc) at 6 cm. We used the KARMA tool KPVSLICE to estimate the SNR J0527–6549 extension at (6 cm image) the 3σ noise level (0.45 mJy) along the major (NE) (Fig. 4) and minor (NW) axis (PA=45°). We note that our estimate of the major diameter is significantly larger (∼34″) than the previously measured by Mathewson et al. (1983). We attribute this to the SNR NE extension detected in [O III] that was not seen in any other optical wavebands (see Fig. 3; right panel). However, our measurements are in a better agreement with radio diameters (61×56 pc) previously reported by Mills et al. (1984). The MCELS images are showing a particularly strong [O III] emission around the North, North East (NE) and North West (NW) part of the shell. Especially, in the NW direction where SNR J0527–6549 extends to $325'' \pm 4''$ (78±1 pc) diameter which is significantly more than at radio or other optical frequencies (Fig. 3; right panel). Also, we note a prominent Hα emission towards the southern part of SNR that is probably causing a shell brightening at that end. Overall, the optical and radio-continuum emissions follow each other.
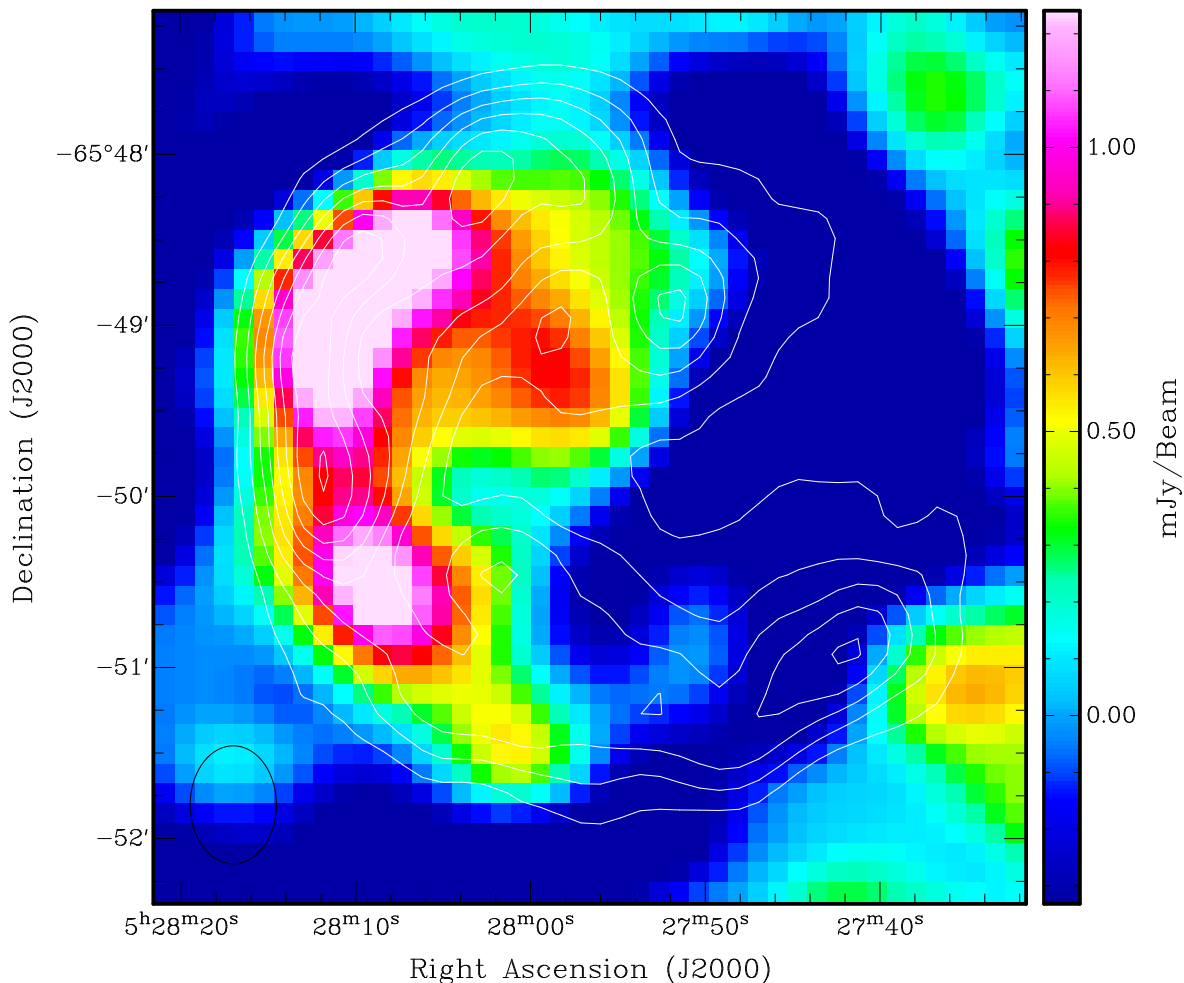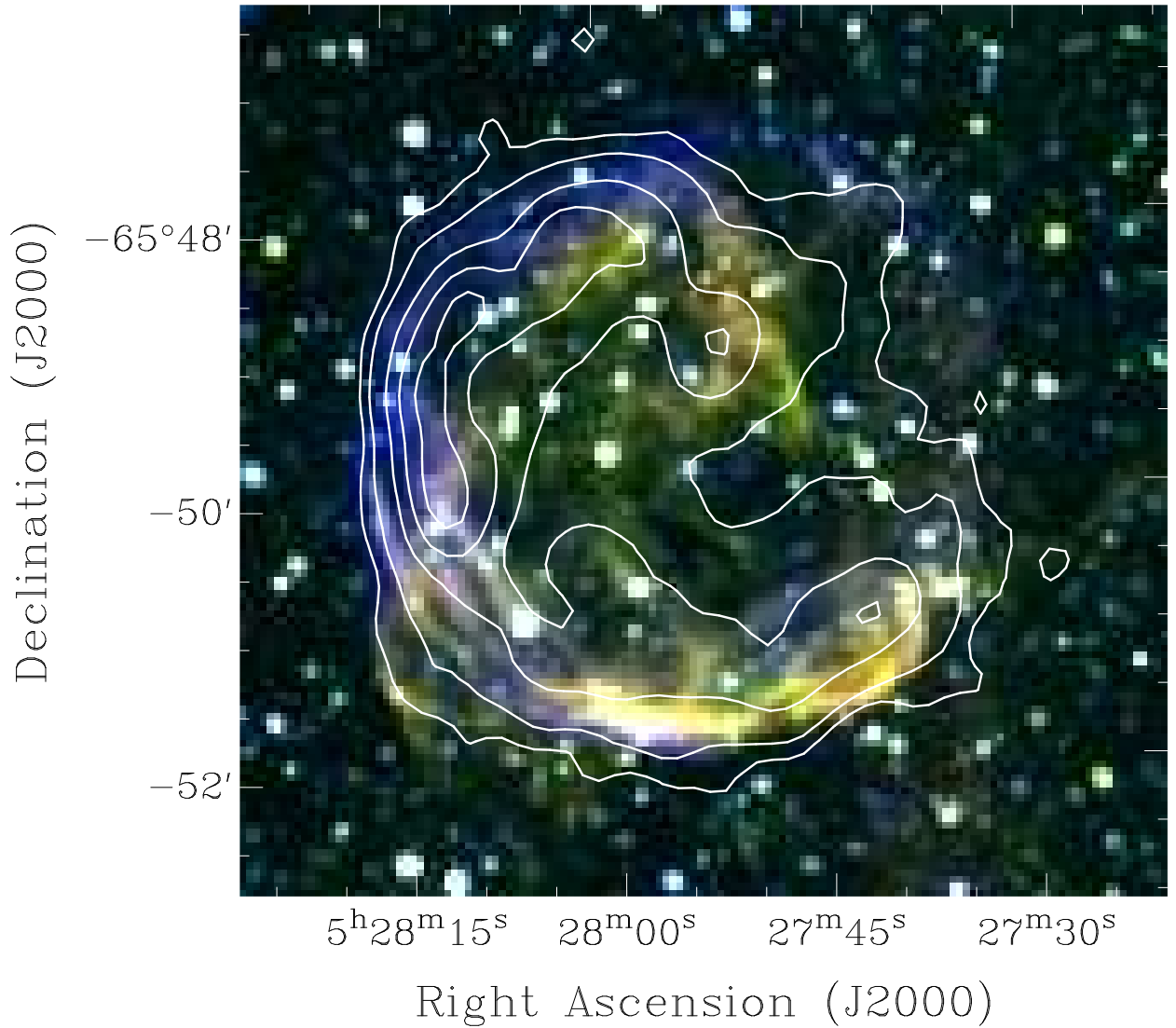
Fig. 1. *ATCA observations of SNR J0527–6549 at 3 cm (8.6 GHz) overlaid with 6 cm (4.8 GHz) contours. The contours are 3, 5, 7, 9, 11, 13, 15 and 17σ. The black circle in the lower left corner represents the synthesised beamwidth (at 6 cm) of 41.4″×30.3″. The sidebar quantifies the pixel map and its units are mJy/beam.*

In order to estimate the spectral energy distribution for this object, we use our new integrated flux density measurements at various radio frequencies with 408 MHz measurement by Mathewson et al. (1983), 843 MHz measurement by Mills et al. (1984) as well as at 1400 MHz (from the mosaics presented by Filipović et al. (2009) and Hughes et al. (2007)). We list these flux density measurements at various frequencies in Table 1 and then plot the SNR J0527–6549 spectral index (α) in (Fig. 5). The overall radio-continuum spectral index of SNR J0527–6549 is unusually steep (α=–0.92±0.11) given that this is most likely an older (evolved) SNR, due to its rather large size of ∼66 pc. Usually, a steep gradient like this would suggest a much younger and energetic SNR. However, in this case, the steepness can be contributed to the fact of missing short spacings at higher radio-continuum frequencies (4800 and 8640 MHz) and, therefore, a missing flux. Specifically at 3 cm (where the ATCA primary beam is ∼300″) this SNR edges would be positioned close to the primary beam boundary where the flux tends to significantly uncertain. We also note that this may indicate that a simple model does not accurately describe the data, and that a higher order model is needed. This is not unusual, given that several other Magellanic Clouds SNR's exhibit this "curved" spectra (Crawford et al. 2008b). Noting the breakdown of the power law fit at shorter wavelengths, we decomposed the spectral index estimate into two components, one (α_1) between 73 and 20 cm, and the other (α_2) between 6 and 3 cm. The first component, α_1= – 0.51±0.08, is a very good fit and typical of an SNR, whereas the second, α_2=–1.60±0.34, is a poor fit, and indicates that non-thermal emission can be described by different populations of electrons with different energy indices. Although the low flux at 3 cm (and to a lesser extent at 6 cm) could cause the large deviations, an underestimate of up to ∼50% would still lead to a "curved" spectrum.

Table 1. Integrated Flux Density of SNR J0527–6549.

ν (MHz)	λ (cm)	R.M.S (mJy)	Beam Size ($''$)	S_{Total} (mJy)	Reference
408	73	—	156×156	260	Mathewson et al. (1983)
843	36	1.5	43×43	166	Mills et al. (1984)
1400	20	1.5	45.0×45.0	140	This Work
4800	6	0.15	41.4×30.2	38.4	This Work
8640	3	0.17	22.9×16.5	15.0	This Work

Fig. 2. *MCELS composite optical image (RGB =Hα,[S II],[O III]) of SNR J0527–6549 overlaid with 6 cm contours. The contours are 1, 3, 7, 11 and 15σ.*

Such a curved spectrum, shown in Fig. 5, can be explained using the so-called diffuse shock acceleration (DSA) theory coupled with the effect of synchrotron losses within the finite emission region. If the thin region near the shock discontinuity is not resolved by the telescope beam, the observed emission includes some flux from electrons which have been diffused away from the place of effective acceleration and lose a significant amount of energy via the synchrotron emission. As these losses are more severe for higher energy electrons, we expect this to steepen the observed synchrotron spectrum. For details see Heavens and Meisenheimer (1987), Longair (2000, and references therein).

The linear polarization images for each frequency were created using parameters Q and U (Fig. 6). The 6 cm image reveals some strong linear polarization, greater than with various other LMC SNRs (Bojičić et al. 2007, Crawford et al. 2008a,b, Čajko et al. 2009, Crawford et al. 2010). The mean fractional polarisation at 6 cm was calculated using the flux density and polarisation:

$$P = \frac{\sqrt{S_Q^2 + S_U^2}}{S_I} \cdot 100\% \qquad (1)$$

where S_Q, S_U and S_I are integrated intensities for Stokes parameters Q, U and I. Our estimated peak value is 54%±17% at 6 cm and no reliable detection at 3 cm. Along the shell there is a very strong uniform polarisation coinciding with the total peak intensity located at the north-west side of the shell. We note that SNR J0527–6549 exhibits one of the strongest polarisations observed so far in the LMC averaged at approximately 50% (Fig. 6) as would be expected from the non-thermal SNRs. This relatively high level of polarization is (theoretically) expected for an SNR with a radio spectrum of around or less than −0.5 (Rolfs and Wilson 2003). Possibly, this may indicate varied dynamics along the shell. Without reliable polarisation measurements at a second frequency we could not determine the Faraday rotation, and thus cannot deduce the magnetic field strength.
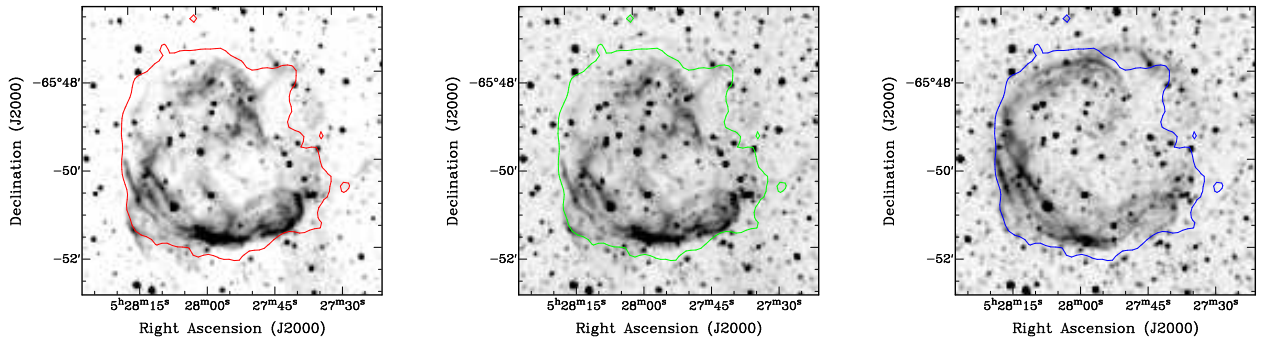

Fig. 3. *MCELS optical images (Hα (Left), [S ɪɪ] (Middle), [O ɪɪɪ] (Right)) of SNR J0527–6549 overlaid with a single 1σ 6 cm contour.*
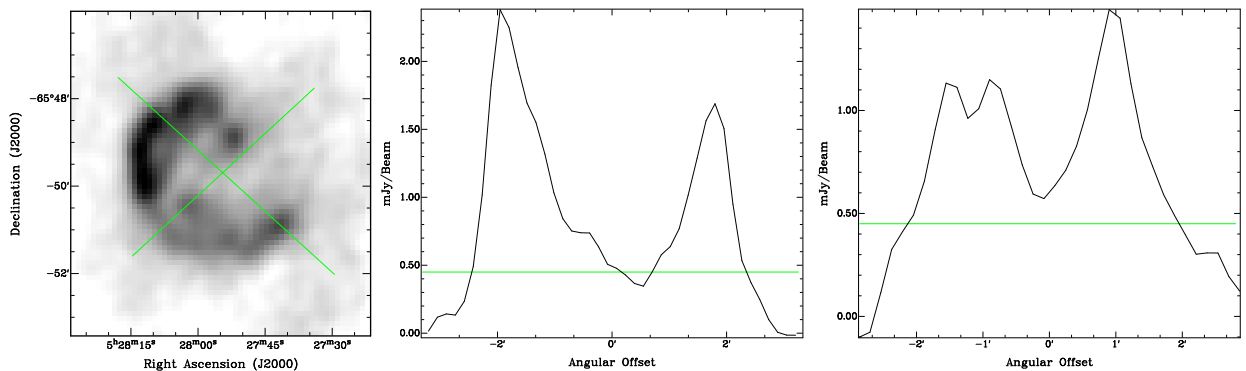

Fig. 4. *The left image shows the major and minor axis, with the major axis starting at the NW corner and the minor axis starting at the SW corner. The center image shows the I-Profile of the major axis with the 3σ line shown. The right image shows the I-Profile of the minor axis with the 3σ line shown.*
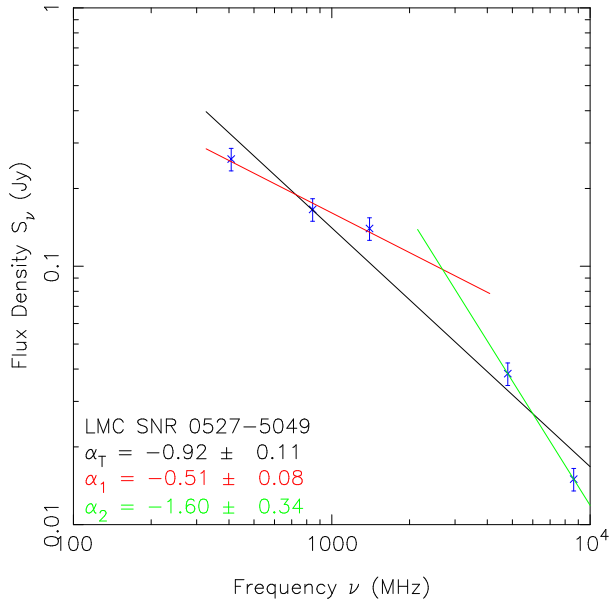
47

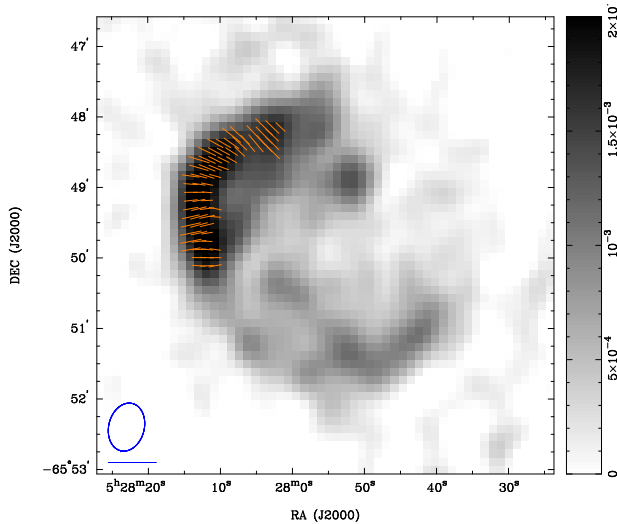**Fig.** **5.** *Radio-continuum spectrum of SNR J0527–6549.*

Fig. 6. *ATCA observations of SNR J0527–6549 at 6 cm (4.8 GHz). The blue circle in the lower left corner represents the synthesised beamwidth of $41.4'' \times 30.3''$, and the blue line below the circle is the polarization vector of 100%. The sidebar quantifies the pixel map and its units are Jy/beam.*

4. CONCLUSION

We conducted the highest resolution radio-continuum and optical observations to date of SNR J0527–6549. From this analysis, we confirmed this object as a bona-fide SNR with a relatively large diameter of $271'' \times 240'' \pm 4''$ ($66 \times 58 \pm 1$ pc), a complex spectral index ($\alpha = -0.92 \pm 0.11$), strong polarisation of $\sim 54\% \pm 17\%$, as well as strong circular optical [O III] emission.

REFERENCES

Blair, W. P., Ghavamian, P., Sankrit, R., Danforth, C. W.: 2006, *Astrophys. J. Suppl. Series*, **165**, 480.
Bojičić, I. S., Filipović, M. D., Parker, Q. A., Payne, J. L., Jones, P. A., Reid, W., Kawamura, A., Fukui, Y.: 2007, *Mon. Not. R. Astron. Soc.*, **378**, 1237.
Čajko, K. O., Crawford, E. J., Filipović, M. D.: 2009, *Serb. Astron. J.*, **179**, 55.
Chu, Y-H., Kennicutt, R. C.: 1988, *Astron. J.*, **96**, 1874.
Clarke, J. N., Little, A. G., Mills, B. Y.: 1976, *Aust. J. Phys. Astrophys. Suppl.*, **40**, 1.
Crawford, E. J., Filipović, M. D. and Payne, J. L.: 2008a, *Serb. Astron. J.*, **176**, 59.
Crawford, E. J., Filipović, M. D., De Horta, A. Y., Stootman, F. H., Payne, J. L.: 2008b, *Serb. Astron. J.*, **177**, 61.
Crawford, E. J., Filipović, M. D., Haberl, F., Pietsch, W., Payne, J. L., De Horta, A. Y.: 2010, *Astron. Astrophys.*, **518**, A35.
Davies, R. D., Elliott, K. H., Meaburn, J.: 1976, *Mem. R. Astron. Soc.*, **81**, 89.
Di Benedetto, G. P.: 2008, *Mon. Not. R. Astron. Soc.*, **390**, 1762.
Filipović, M. D., Haynes, R. F., White, G. L., Jones, P. A., Klein, U., Wielebinski, R.: 1995, *Astron. Astrophys. Suppl. Series*, **111**, 331.
Filipović, M. D., White, G. L., Haynes, R. F., Jones, P. A., Meinert, D., Wielebinski, R., Klein, U.: 1996, *Astron. Astrophys. Suppl. Series*, **120**, 77.
Filipović, M. D., Haynes, R. F., White, G. L., Jones, P. A.: 1998a, *Astron. Astrophys. Suppl. Series*, **130**, 421.
Filipović, M. D., Pietsch, W., Haynes, R. F., White, G. L., Jones, P. A., Wielebinski, R., Klein, U., Dennerl, K., Kahabka, P., Lazendić, J. S.: 1998b, *Astron. Astrophys. Suppl. Series*, **127**, 119.
Filipović, M. D., Crawford, E. J., Hughes, A., Leverenz, H., de Horta, A. Y., Payne, J. L., Staveley-Smith, L., Dickel, J. R., Stootman, F. H., White, G. L.: 2009, in van Loon J. T., Oliveira J. M., eds, *IAU Symposium Vol. 256*, PDF8.

Gooch, R.: 2006, Karma Users Manual, ATNF, Sydney.

Haberl, F., Pietsch, W.: 1999, *Astron. Astrophys. Suppl. Series.* **139**, 277.

Heavens, A. F., Meisenheimer, K.: 1987, *Mon. Not. R. Astron. Soc.*, **225**, 335.

Hughes, A., Staveley-Smith, L., Kim, S., Wolleben, M., Filipović, M. D.: 2007, *Mon. Not. R. Astron. Soc.*, **382**, 543.

Long, K. S., Helfand, D. J., Grabelski, D. A.: 1981, *Astrophys. J.*, **248**, 925.

Longair, M. S.: 2000, High Energy Astrophysics (vol. 2), Cambridge University Press.

Mathewson, D. S., Ford, V. L., Dopita, M. A., Tuohy,

I. R., Long, K. S., Helfand, D. J.: 1983, *Astrophys. J. Suppl. Series*, **51**, 345.

Mills, B. Y., Turtle, A. J., Little, A. G., Durdin, J. M.: 1984, *Aust. J. Phys.*, **37**, 321.

Payne, J. L., White, G. L., Filipović, M. D.: 2008, *Mon. Not. R. Astron. Soc.*, **383**, 1175.

Rolfs, K., Wilson, T.: 2003, "Tools of Radio Astronomy 4ed.", Springer, Berlin.

Sault, R. J., Killeen, N.: 2010, Miriad Users Guide, ATNF, Sydney.

Sault, R. J., Wieringa, M. H.: 1994, *Astron. Astrophys. Suppl. Series*, **108**, 585.

Smith, C., Points, S., Winkler, P. F.: 2006, *NOAO Newsletter*, **85**, 6.

МУЛТИФРЕКВЕНЦИОНА РАДИО-ПОСМАТРАЊА ОСТАТКА СУПЕРНОВЕ У ВЕЛИКОМ МАГЕЛАНОВОМ ОБЛАКУ. СЛУЧАЈ SNR J0527–6549 (DEM L204)

L. M. Bozzetto, M. D. Filipović, E. J. Crawford, I. S. Bojičić, J. L. Payne,

A. Mendik, B. Wardlaw and A. Y. De Horta

School of Computing and Mathematics, University of Western Sydney
Locked Bag 1797, Penrith South DC, NSW 1797, Australia

E–mail: *m.filipovic@uws.edu.au*

У овој студији представљамо нове ATCA резултате посматрања у радио-континууму за остатак супернове у Великом Магелановом Облаку – SNR J0527–6549. Овај објект је типичан остатак супернове са потковичастом морфологијом. Измерена вредност дијаметра износи D=(66×58)±1 парсека. Ово је један од највећих остатака супернових у Великом Магелановом облаку. Димензије остатка указују да је то старији објект, док је спектрални индекс ($\alpha = -0.92\pm0.11$) веома стрм и повремено се среће код млађих остатака. Детектовали смо висок степен поларизације чак и до 54%±17% (мерења на 6-цм).